JACS
JOURNAL OF THE AMERICAN CHEMICAL SOCIETY

Article

pubs.acs.org/JACS

Multiple Unfolding Pathways of Leucine Binding Protein (LBP) Probed by Single-Molecule Force Spectroscopy (SMFS)

Hema Chandra Kotamarthi, Riddhi Sharma, Satya Narayan, Sayoni Ray, and Sri Rama Koti Ainavarapu*

Department of Chemical Sciences, Tata Institute of Fundamental Research, Homi Bhabha Road, Colaba, Mumbai 400005, India

Supporting Information

ABSTRACT: Experimental studies on the folding and unfolding of large multi-domain proteins are challenging, given the proteins' complex energy landscapes with multiple intermediates. Here, we report a mechanical unfolding study of a 346-residue, two-domain leucine binding protein (LBP) from the bacterial periplasm. Forced unfolding of LBP is a prerequisite for its translocation across the cytoplasmic membrane into the bacterial periplasm. During the mechanical stretching of LBP, we observe that 38% of the unfolding flux followed a two-state pathway, giving rise to a single unfolding force peak at ∼70 pN with an unfolding contour length of 120 nm in constant-velocity single-molecule pulling experiments. The remaining 62% of the unfolding flux followed multiple three-state pathways, with intermediates having unfolding contour lengths in the range ∼20−85 nm. These results suggest that the energy landscape of LBP is complex, with multiple intermediate states, and a large fraction of molecules go through intermediate states during the unfolding process. Furthermore, the presence of the ligand leucine increased the unfolding flux through the two-state pathway from 38% to 65%, indicating the influence of ligand binding on the energy landscape. This study suggests that unfolding through parallel pathways might be a general mechanism for the large two-domain proteins that are translocated to the bacterial periplasmic space.

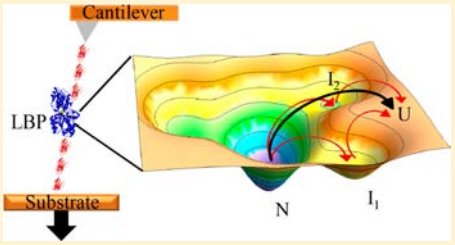

INTRODUCTION

Unfolding of proteins is a prerequisite in cellular processes such as protein translocation and degradation.[1] In such cases, the unfolding is achieved by application of mechanical forces exerted by the ATP-dependent molecular motors.[2] Hence, application of stretching forces to proteins *in vitro* can provide a detailed understanding of the mechanical response as well as the unfolding pathways of proteins. It has recently been shown that the mechanical denaturation pathway of protein substrates by an ATP-dependent unfoldase is same as that given by the protein energy landscapes measured in single-molecule experiments.[3] Protein unfolding and folding in general are complex phenomena governed by the underlying energy landscape. Many theoretical studies have predicted that protein energy landscapes are rugged and proteins can take multiple pathways during transition from the folded to the unfolded state and vice versa.[4,5] It has also been proposed that proteins on such energy landscape can follow general kinetic partitioning mechanism while taking different pathways.[6,7] Although there have been many experimental studies on the unfolding and folding of single-domain globular proteins, very little is known about the multi-domain proteins because of their complexity.[8−13] Bioinformatics analysis of genome sequences have revealed that about two-thirds of proteins in prokaryotes consist of multiple domains, which makes the understanding of multi-domain proteins even more important.[14,15] It is generally assumed that the multi-domain proteins have complex unfolding pathways involving one or more intermediates *en route* to the unfolded state.[11,16,17] Recent theoretical and experimental studies on multi-domain proteins have highlighted the relevance of protein energy landscapes with many intermediates and parallel folding pathways.[13,18−20] Here, we report a detailed study on the mechanical unfolding of a physiologically relevant two-domain protein using single-molecule force spectroscopy (SMFS).

SMFS is an atomic force microscope-based technique that applies stretching forces to single protein molecules and measures their response in terms of mechanical stability.[21] In the past decade, SMFS has emerged as a powerful technique for detailed understanding of the unfolding and folding of proteins at the single-molecule level.[21−29] In the mechanical unfolding experiments, the stretching force acts as a denaturant analogous to chemicals in chemical denaturation and temperature in thermal unfolding. In these experiments, the force required to unfold a protein indicates its mechanical stability while the unfolding contour length serves as a reaction coordinate for the unfolding process. This technique is also proven to be useful in characterizing the intermediate states in protein unfolding.[22,30,31] More importantly, mechanical unfolding of proteins by SMFS mimics the unfolding processes that occur *in vivo* during the translocation across membranes or protein degradation.[3] In this regard, study of mechanical unfolding of periplasmic binding proteins (PBPs) would not only serve as a model system for studying the role of mechanical forces on proteins which undergo translocation across membranes but also give insights into the unfolding energy landscape of large two-domain proteins.

Received: June 20, 2013
Published: September 9, 2013

   dx.doi.org/10.1021/ja406238q | J. Am. Chem. Soc. 2013, 135, 14768−14774

In Gram-negative bacteria, PBPs are the primary receptors for nutrient uptake and are responsible for chemotactic responses. PBPs are large two-domain proteins with molecular mass in the range ~25−60 kDa, and they can bind one or more types of ligands with binding affinity ~0.01−1 μM.[32] These proteins are synthesized in cytosol and then undergo translocation into the periplasm. Forced unfolding of these proteins prior to their insertion into the narrow pores of protein channels in the membrane is a key step in the translocation process. Here, we chose leucine binding protein (LBP), which belongs to the class of periplasmic binding proteins (PBP), to investigate its unfolding pathways. This study would provide insights into the mechanical unfolding pathways of multi-domain proteins. LBP is a large, 346-residue, two-domain leucine-transporting protein in the bacterial periplasmic space. It has a mixed α/β structure as shown in Figure 1. Its structure has a "clam-like" shape with the ligand

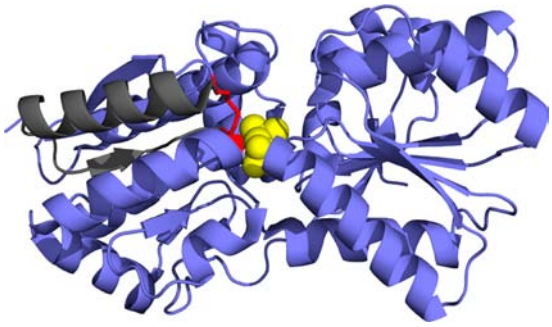

Figure 1. Structure of leucine binding protein (LBP). LBP has a mixed α/β structure with a clam-like shape. Leucine (indicated in yellow) binds in the cleft between the two domains. The residues between cys53 and cys78 (indicated in gray) are locked by a disulfide bond and are sequestered from mechanical unraveling in oxidized conditions. The disulfide bond is indicated in red.

binding site in the cleft formed by the two domains. It has open and close conformations depending on the ligand binding state.[33] LBP has been observed to unfold via a two-state pathway in bulk denaturation experiments.[34] In this study we set out to explore the unfolding phenomena of LBP using SMFS.

EXPERIMENTAL SECTION

Construction of Chimeric $(I27)_3$-LBP-$(I27)_3$ Gene. A plasmid containing heptameric I27 gene, (pQE80L$(I27)_7$), was constructed using an iterative cloning procedure as described previously by Carrion-Vazquez et al.[24] In this plasmid, a set of unique restriction sites were engineered such that the cDNA coding for the fourth I27 gene is flanked by the restriction sites for the enzymes *Sac*I and *Nhe*I at 5′ and 3′ ends, respectively, so as to facilitate the insertion of any other gene of interest in its place. The cDNA coding for the LBP was amplified by PCR to incorporate *Sac*I and *Nhe*I sites at 5′ and 3′ ends, respectively, and digested at these restriction sites and purified to get the LBP insert. The plasmid, (pQE80L$(I27)_7$), was digested with *Sac*I and *Nhe*I to remove the central I27 gene and the resulting vector was ligated with the LBP insert so that the resulting plasmid will have our gene of interest, i.e., $(I27)_3$-LBP-$(I27)_3$.

Protein Expression and Purification. The plasmid with cDNA coding for $(I27)_3$-LBP-$(I27)_3$ was transformed into BLRDE3 strain of *E. coli*. The protein expression was induced by adding 1 mM IPTG after the OD_{600} of the bacterial culture reached 0.6. The purification was done using Ni^{2+} ion affinity chromatography. After the protein was bound to the Ni^{2+} coated agarose beads, the beads were washed with PBS (pH 7.4), and the protein was eluted with the same buffer containing 250 mM imidazole. The proteins were further purified using Superdex200 column (GE Healthcare) on a FPLC system. The holo form of the protein was made by adding leucine to the protein solution such that the final concentration of leucine is 5 mM. Reduced form of the protein was made by incubating the protein with a disulfide reducing agent, tris(2-carboxyethyl)phosphine hydrochloride (TCEP), at a concentration of 5 mM.

Single-Molecule Force Spectroscopy (SMFS). Single-molecule pulling experiments were performed on a custom-built atomic force microscope, whose details are given elsewhere.[22,29] Briefly, a 50 μL of protein solution was added onto a gold-coated glass coverslip. The cantilever was calibrated in protein solution prior to recording force-versus-extension traces, and its spring constant was calculated using the equipartition theorem.[35] The spring constant was found to be ~40 pN/nm.

RESULTS

Mechanical Unfolding of holo LBP. SMFS measurements were performed on the holo form of the chimeric polyprotein $(I27)_3$-LBP-$(I27)_3$ with 5 mM leucine in solution and in reducing conditions. The results are shown in Figure 2. The pulling experiments were carried out at a speed of 1000 nm/s, and force-versus-extension (FX) traces were recorded. A typical FX trace of the polyprotein is shown in Figure 2B. The well-characterized I27 protein acts as a mechanical fingerprint in identifying the single-molecules in FX traces.[36] As LBP protein is flanked by three I27s on either side, observation of four or more I27s in a single FX trace guarantees that LBP has been mechanically stretched in the pulling experiment. The FX traces were fitted to the worm-like chain (WLC) model to obtain the change in contour length (ΔL_c) associated with each force peak.[37]

A sawtooth pattern with ΔL_c ~28 nm and unfolding force ~200 pN serves as the fingerprint of I27s in the chimeric protein. The peak prior to the first I27 peak with a ΔL_c ~120 nm is due to the unfolding of LBP upon mechanical stretching. LBP consists of 346 residues and its expected contour length would be 120 nm (= 346aa × 0.36 nm/aa − 5 nm), where 5 nm is the N−C distance in the protein from its X-ray structure (PDB code 1USG). The experimentally measured ΔL_c of LBP is the same as that of the expected value confirming that the force peak preceding all the I27s is indeed the result of the mechanical unfolding of LBP. The average unfolding force of LBP (~70 pN) measured in the experiment is much lower than that of I27. This also suggests that the unfolding force peak of LBP must precede the I27 sawtooth, in spite of its positioning in the middle of the chimeric polyprotein, as observed in all the FX traces. Furthermore, the observation of only a single force peak also indicates that LBP unfolds in a two-state (N−U), all-or-none manner. Distributions of the unfolding forces and the change in contour length are shown in Figure 2C,D.

Multiple Unfolding Pathways of LBP. A large fraction (~65%) of polyproteins exhibited FX traces of the kind shown in Figure 2B with a single unfolding force peak for LBP. However, the remaining fraction (~35%) showed two force peaks prior to the unfolding sawtooth pattern of I27s (Figure 3A). The I27 unfolding characteristics are the same as those shown in Figure 2B. In Figure 3A, the FX trace at the top shows a single force peak with ΔL_c ~120 nm, whereas the second FX trace from the top shows two force peaks with ΔL_c values of 49 and 73 nm. In the second FX trace, the sum of the two ΔL_c values is 122 nm (= 49 nm +73 nm), indicating that the LBP in this case unfolded along a three-state pathway (N−I−U), where the second peak with ΔL_c ~73 nm corresponds to

dx.doi.org/10.1021/ja406238q | J. Am. Chem. Soc. 2013, 135, 14768−14774

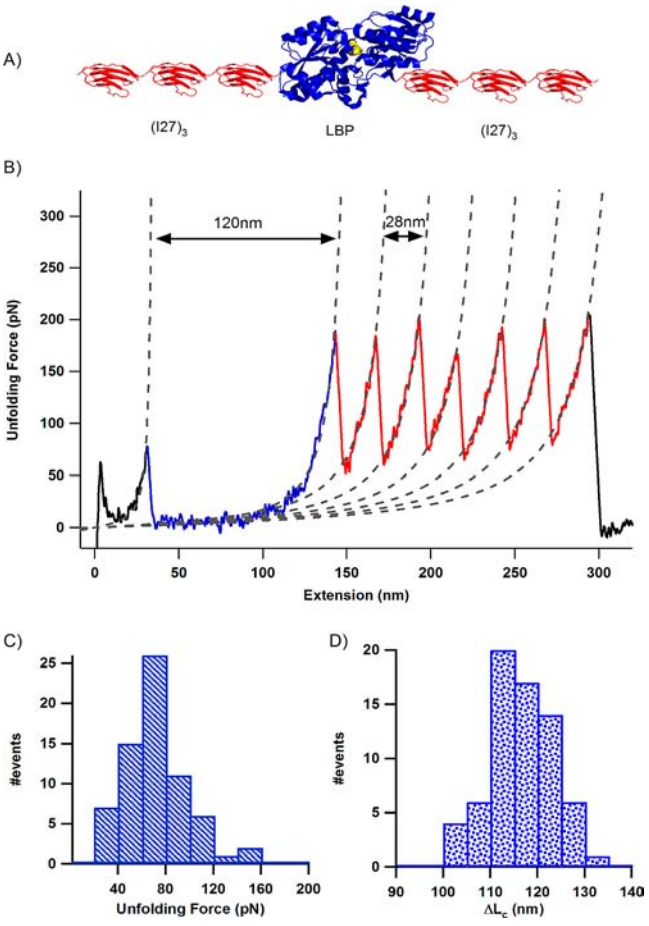

Figure 2. (A) Cartoon picture of chimeric polyprotein $(I27)_3$-LBP-$(I27)_3$. (B) A representative force-versus-extension (FX) trace of the LBP chimera in presence of 5 mM leucine and TCEP at a pulling speed of 1000 nm/s. Force peaks in the trace were fitted to the WLC model (gray dotted lines) to obtain the contour length increment (ΔL_c). The force peaks with ΔL_c ~28 nm correspond to the unfolding of I27 (colored in red) whereas the force peak with ΔL_c ~120 nm corresponds to the all-or-none unfolding of LBP (colored in blue). (C) Distribution of the unfolding forces of LBP. The unfolding force of LBP is 70 ± 26 pN (average ± SD). (D) Distribution of the contour length increments of LBP upon unfolding. The change in contour length is 116 ± 7 nm (average ± SD).

the unraveling of an intermediate of LBP to the denatured state. In the analysis of FX traces for assigning them to three-state pathways, force peaks were identified as intermediates only if they could be fitted to the WLC model and have a peak force above the instrumental noise (~15 pN). The experimental data indicates that LBP follows kinetic partitioning during the mechanical unfolding in which some population take a two-state pathway (N−U) while the others follow a three-state pathway (N−I−U). Kinetic partitioning in single-molecule mechanical unfolding studies was observed earlier for maltose binding protein (MBP) and T4 lysozyme.[22,38] However, for the LBP molecules that are unfolding along the three-state pathway, the ΔL_c values of the two peaks are not constant but distributed over a wide range.

For example, in Figure 3A, the third FX trace has force peaks with ΔL_c values of 89 and 28 nm, which are different from the second FX trace. Although the ΔL_c values of these two peaks are highly varied, their sum is ~120 nm as can be seen from the scatter plot in Figure 3B. The ΔL_c of the LBP intermediate (from the second force peak to the first I27 force peak) and the sum ΔL_c of LBP (from the first force peak to the first I27 force peak) versus their unfolding force is plotted Figure 3B. The ΔL_c versus unfolding force for the two-state pathway is also shown in Figure 3B. The average unfolding forces of the main peak and the intermediate peak are similar (~70 pN) suggesting that the main unfolding event (N−U or N−I) and the intermediate unfolding events (I−U) processes have similar mechanical stabilities. Distributions of the unfolding forces and the ΔL_c of main and intermediate force peaks of LBP are given in the Supporting Information (Figure S1). No apparent correlation was found between the unfolding forces of the main and the intermediate peaks (Figure S2). Although the sum ΔL_c is ~120 nm, a large spread (14−95 nm) in the ΔL_c of the intermediates suggest that the intermediates differ widely in size as well as structure. It is possible that LBP after crossing the initial unfolding barrier, which results in the first or main force peak, gets trapped in different kinetic traps or intermediates in which molecules are mechanically stable at least in the time scale of milliseconds and further stretching is needed to completely unfold the molecule, which results in the second or intermediate force peak. Our results suggest not only that LBP goes through parallel pathways (two-state and three-state) but also that the three-state pathways are diverse in nature.

Mechanical Unfolding Properties of LBP in Oxidizing Conditions. LBP has a disulfide bond in its structure between cysteines at 53 and 78 as shown in Figure 1. The residues between these cysteines would be shielded from the mechanical force because of the disulfide linkage present in oxidizing conditions.[39] In order to test this hypothesis, we have performed pulling experiments on both apo and holo forms of LBP chimera in oxidizing conditions where no reducing agent was added and the cysteines were allowed to form the disulfide bond.

Representative FX traces of LBP under oxidizing conditions are given in Figure 4A. We observed that LBP unfolded via both two-state and three-state pathways in the oxidizing conditions as well. There are two cysteines in I27 which do not form disulfide bond as they are far apart in the structure and hence the signature of I27 in FX trances obtained in oxidizing conditions was not affected.[40] The FX traces were fitted to the WLC model to extract the ΔL_c values of force peaks. The first FX trace in Figure 4A is shown just for comparison and was obtained under reducing conditions. The other two FX traces were obtained under oxidizing conditions and clearly show that the unfolding of LBP gives rise to either one or two force peaks indicating kinetic partitioning. The sum ΔL_c is ~110 nm, and the ΔL_c of intermediates is again a large spread (20−90 nm) as in the case of reduced LBP. The expected ΔL_c of oxidized LBP with the cys53−cys78 disulfide bond sequestering 25 amino acids is ~110 nm (= 321 × 0.36 nm − 5 nm). An overlay of the sum ΔL_c distribution under oxidizing and reducing conditions is shown in Figure 4B. The unfolding forces of the main peak as well as the intermediate peak in both oxidizing and reducing forms are largely similar (Table 1). The unfolding FX traces in oxidizing conditions show that the shielding of 25 residues between cys53 and cys78 residues has no effect on the mechanical unfolding pathway of LBP and it still follows two-state as well as multiple three-state pathways. The unfolding force and the ΔL_c distributions for holo LBP under oxidizing conditions are given in Figure S3.

Mechanical Stability of apo LBP. In order to see if there are any differences in the mechanical unfolding properties of

dx.doi.org/10.1021/ja406238q | J. Am. Chem. Soc. 2013, 135, 14768−14774

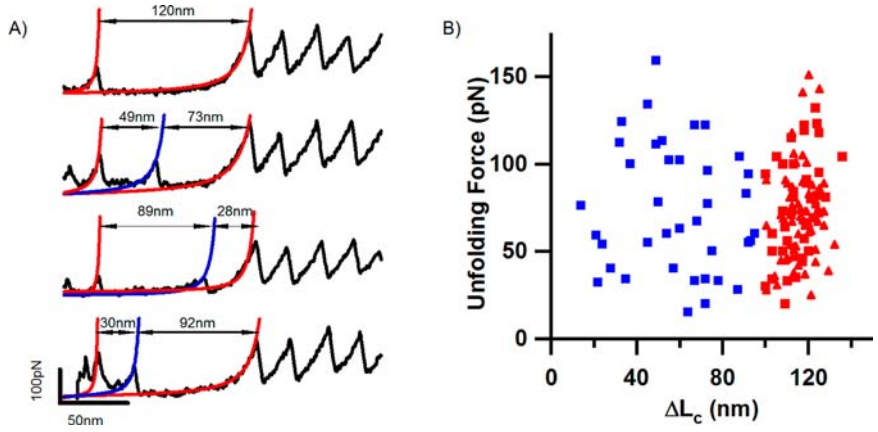

Figure 3. (A) Representative FX traces of LBP showing intermediates with widely varying ΔL_c. The first trace shows that the molecule unfolded in a two-state pathway without any intermediate. Remaining FX traces show that LBP unfolded in three-state pathways with intermediates having different ΔL_c values. The WLC model fits are shown for LBP main peak (red), LBP intermediate peak (blue), and the first I27 peak (red). (B) Scatter plot showing the unfolding force versus ΔL_c of intermediate peak (blue squares) and main peak (red squares) for the three-state pathway, and unfolding force versus ΔL_c for the two-state pathway (red triangles). The ΔL_c of intermediates (blue squares) is between the intermediate peak and the first I27 peak. The sum ΔL_c of LBP (red squares) from the LBP main peak to the first I27 peak is ~120 nm for all the traces. See text and Table 1 for more details.

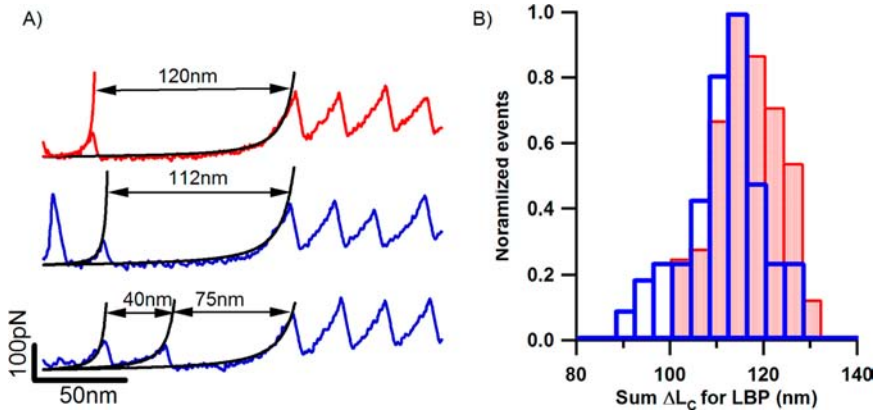

Figure 4. Comparison of the mechanical unfolding of LBP in oxidizing and reducing conditions. (A) The first FX trace is obtained under reducing conditions and has a ΔL_c ~120 nm. The second FX trace is obtained under oxidizing conditions and the ΔL_c has decreased to ~112 nm due to the sequestration of 25 residues between cys53 and cys78. The third FX trace is of LBP in oxidizing conditions showing that it unfolds in a three-state manner and the disulfide sequestration has no effect on the unfolding pathways of LBP. (B) Histograms of the sum ΔL_c of LBP in oxidizing (blue) and reducing (red) conditions. See text and Table 1 for more details.

Table 1. Mechanical Properties of LBP

	main peak[a]		intermediate peak		
condition	force (pN)[b]	ΔL_c (nm)[b]	force (pN)[b]	ΔL_c(nm)[c]	% unfolding flux through intermediate[d]
LBP + Leu + TCEP	72 ± 28 (N = 106)	115 ± 10	72 ± 36	14–95	35 ± 5
LBP + TCEP	82 ± 35 (N = 30)	117 ± 15	62 ± 23	25–84	62 ± 9
LBP + Leu	78 ± 31 (N = 78)	110 ± 11	66 ± 26	15–84	36 ± 6
LBP	76 ± 34 (N = 60)	108 ± 15	70 ± 31	21–93	57 ± 6

[a]Data for the main force peak is from both two-state and three-state pathways. For the three-state pathways, the ΔL_c of the main peak is with respect to the first I27 unfolding force peak. [b]The errors are SD. [c]The range of ΔL_c. [d]Percentage of unfolding flux through intermediate = (no. of FX traces with intermediate/total no. of FX traces) x 100. The errors are SE, calculated using the bootstrap method.[22,41]

LBP in the absence and presence of the ligand, we have also performed pulling experiments in the absence of leucine. The unfolding mechanism of apo LBP is similar to that of holo LBP, which means LBP follows multiple pathways with some molecules unfolding via the two-state pathway (N–U) while the remaining follow multiple three-state pathways (N–I–U). The ΔL_c of the intermediate again has a large spread, while the sum ΔL_c is ~120 nm. The average unfolding force of the main unfolding event is ~75 pN and that of the intermediate is ~66 pN suggesting that the absence of the ligand does not affect the mechanical stability of LBP. Distributions of the unfolding forces and the ΔL_c for the main peak (first peak) and the intermediate peak (second peak) are given in Figure S4. Although the unfolding properties of LBP are the same in both apo and holo forms, the propensity of the molecules (unfolding flux) going through the intermediate enhances from 35% to

dx.doi.org/10.1021/ja406238q | J. Am. Chem. Soc. 2013, 135, 14768–14774

62% in the absence of ligand under reducing conditions and from 36% to 57% under oxidizing conditions (Figure 5). This

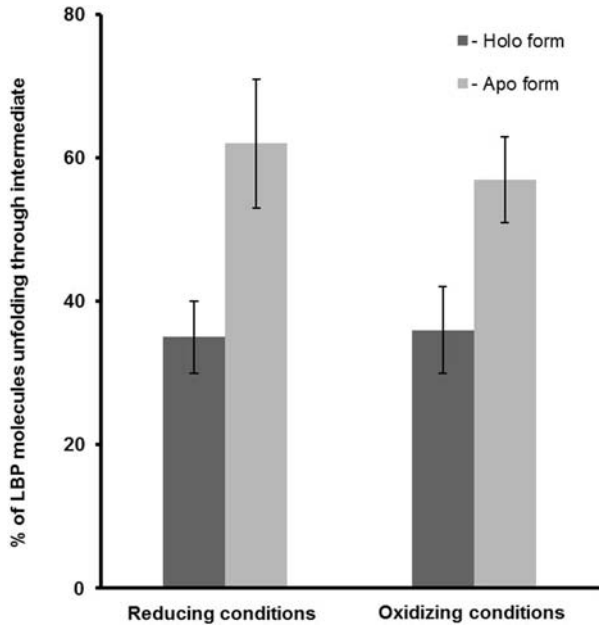

Figure 5. Bar diagram showing the percentage of molecules (unfolding flux) going through intermediates. In the absence of ligand, the unfolding flux is high through three-state unfolding pathways. In the absence of ligand, the unfolding flux through intermediates increases from 35% to 62% (p-value $\leq$ 0.01) under reducing conditions and from 36% to 57% (p-value $\leq$ 0.02) under oxidizing conditions, indicating a greater diversity in its unfolding pathways. The error bars are the SE, calculated using the bootstrap method (see Table 1).

clearly indicates that there is a greater diversity in the unfolding pathways of LBP in the absence of ligand. The p-values between apo and holo forms for the percentages of unfolding flux through intermediates in reducing and oxidizing conditions are 0.01 and 0.02, respectively, which means the observed differences with ligand binding are statistically significant. On the other hand, the p-values between oxidizing and reducing conditions are 0.82 for apo and 0.99 for holo LBP, which indicates that the presence of disulfide bond is not crucial in dictating the unfolding pathways. Hence, we can conclude that there is a significant effect of ligand binding on the unfolding pathways of LBP and its effect is similar in both oxidizing conditions and reducing conditions. The unfolding forces and the ΔL_c values of the main and intermediate peaks of LBP under all conditions are given in Table 1.

DISCUSSION

Periplasmic Binding Proteins Show Complexity in Mechanical Unfolding. Our single-molecule study shows that LBP follows a kinetic partitioning mechanism between a two-state and multiple three-state pathways, under forced unfolding conditions. Interestingly, the three-state pathways are diverse in nature as the observed intermediates were shown to have different contour length increments. This kinetic partitioning between the pathways could be either due to inherent ruggedness in the energy landscape or due to heterogeneity in the initial folded conformers. In order to test this hypothesis, we have performed many stretch−relax−restretch cycles on the same protein. The traces are shown in Figure S5. Although the I27s refolded, LBP did not refold within the observation time and detached from tip or surface before it refolded. Therefore, we cannot conclude whether the observed multiple pathways are due to any heterogeneity in the initial conformations or due to ruggedness in the landscape. However, our earlier studies on MBP have clearly shown that the multiple pathways during the mechanical unfolding are intrinsic to the energy landscape and are not due to the conformational heterogeneity of the native state.[22] Hence, it is highly likely that the multiple pathways of LBP might also be due to the inherent complexity of the energy landscape rather than due to the native state conformational heterogeneity, as both MBP and LBP belong to the same class (i.e., PBPs) and have similar function. Although kinetic partitioning seems to be a common feature of PBPs, its specific details might still depend on the detailed connectivity of secondary structural elements in the tertiary structure. This is already evident from the comparison of LBP and MBP, where the former shows multiple pathways but the latter has just two pathways.

Multiple Unfolding Pathways of Multi-domain Proteins. The energy landscape theory based on statistical physics models predict that the proteins need not always take a definite pathway during their transition from the folded compact structure to the unfolded structure but they can take multitude of pathways.[4,42] Many bulk experimental results have shown that proteins do unfold and fold in multiple parallel pathways.[8,9,17,43] Intermediates of LBP during different pathways could be due to the protein getting trapped in different local minima after crossing the main unfolding energy barrier as represented in Figure 6. Kinetic partitioning has earlier been

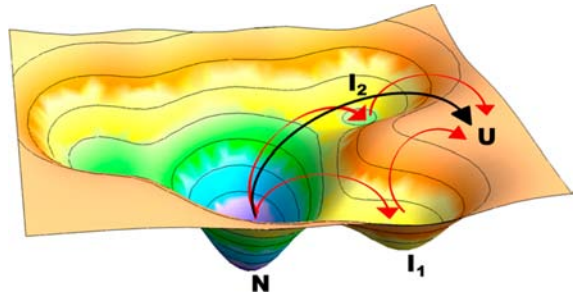

Figure 6. Cartoon energy landscape showing the multiple pathways that LBP follows during mechanical unfolding. LBP not only unfolds along a two-state pathway (black arrow) from native (N) to unfolded (U) state, but also follows many three-state pathways (red arrows) from native (N) to intermediate (I_1, $I2$, ...) to unfolded (U) state. LBP unfolds via parallel pathways by a kinetic partitioning mechanism.

observed for other proteins by SMFS.[22,38,44−47] T4 lysozyme (T4L) has been shown to follow similar mechanical unfolding pathways by kinetic partitioning mechanism: Peng et al.[38] showed that T4L unfolds by multiple distinct unfolding pathways, where the majority unfolds in an all-or-none fashion exhibiting two-state pathway and the others in three-state manner without a well-defined route but displaying diversity in unfolding pathways. LBP is similar to this case but the proportion of molecules going through three-state pathways is much higher for LBP. A recent study on three-domain adenylate kinase exhibited coexistence of multiple intersecting folding pathways associated with a complex energy landscape as characterized in single-molecule fluorescence studies.[18] Theoretical investigations on a four-domain DNA polymerase IV (DPO4) from *Sulfolobus solfataricus* revealed diverse parallel

dx.doi.org/10.1021/ja406238q | J. Am. Chem. Soc. 2013, 135, 14768−14774

folding pathways.[20] The study reported here, along with these earlier reports, gives strong evidence that the energy landscape of multi-domain proteins is complex and multiple energy minima on it give rise to multiple-pathways for the protein to choose during its conformational transitions from the folded to the unfolded state and vice versa.

Implications of the Energy Landscape of LBP in Protein Translocation. Recent studies on ATP-dependent bacterial protease ClpXP have shown that the unfolding mechanism of substrate proteins by the unfoldase ClpX is largely determined by the energy landscape of the substrate protein obtained in SMFS experiments.[3] Interestingly, the intermediate observed in the ClpX mediated unfolding of GFP is identical to that present in the unfolding pathway characterized in the SMFS experiment. This suggests that the energy landscape of LBP would be highly relevant in terms of the unfolding of LBP prior to protein translocation. Also the ClpX unfoldase is shown to generate mechanical forces, albeit at very low pulling rate (5 orders of magnitude smaller) than that of SMFS, to unfold the substrates whose mechanical strength is ∼100 pN as measured by SMFS. Interestingly, the unfolding forces of LBP (<100 pN) measured here are also within the range that could be targeted by ClpX unfoldase.

Ligand-Modulated Unfolding Pathways of PBPs. The effect of ligand binding has also been emphasized in our study. Unlike many small single-domain proteins where the ligand binding increases the protein mechanical strength,[26,48] the ligand has no effect on the unfolding force of LBP but has influence on the unfolding pathway. Ligand binding enhanced the flux through the two-state pathway at the expense of the other three-state pathways. This is an indication of the ligand binding modulated change in the unfolding energy landscape. However, leucine binding has no effect on the unfolding force as the ligand binding site, which is in the cleft between the two domains, is far from the N- and C-termini along which the stretching force is applied. Also, the residues locked by the disulfide bridge have minimal role in the stability and the unfolding pathways of LBP as observed from the studies in oxidizing conditions. Earlier reports on the mechanical stability of MBP and I27 with engineered disulfide bonds have shown that the sequestration by disulfide locking does not influence the mechanical stability of these proteins.[31,39] In our earlier study on MBP, it was shown that ligands maltose and maltotriose modulated the unfolding flux along the three-state pathway.[22]

Mechanical unfolding of LBP differs from that of MBP in two ways. First, MBP has been shown to go through a single three-state pathway whereas LBP follows multiple three-state pathways, revealing the complexity of LBP unfolding. Second, the percentage of unfolding flux influenced by ligand is much more in the case of LBP (>25%) than that of MBP (∼15%).

CONCLUSION

We have studied the mechanical unfolding of LBP and found that it unfolds via parallel pathways: a single two-state pathway and multiple three-state pathways. Furthermore, leucine binding reduced the propensity of LBP to go through intermediates. From the current study on LBP along with earlier reports on MBP, it can be concluded that the two-domain PBPs exhibit kinetic partitioning and ligand binding influences their unfolding pathways. We anticipate the experimental studies on the energy landscape and the mechanical unfolding pathways of LBP will further our understanding of the protein translocation across the bacterial periplasm.

ASSOCIATED CONTENT

Supporting Information

Histograms showing distributions of the unfolding forces and the contour length increments of holo LBP in reducing and oxidizing conditions and apo LBP in reducing conditions; correlation plot of unfolding forces of the main and intermediate peaks of holo LBP under reducing conditions; refolding FX traces of LBP chimera. This material is available free of charge via the Internet at http://pubs.acs.org.

AUTHOR INFORMATION

Corresponding Author

koti@tifr.res.in

Notes

The authors declare no competing financial interest.

ACKNOWLEDGMENTS

The authors thank TIFR for financial support and Prof. R. Varadarajan (IISc, Bangalore) for the LBP gene. The authors acknowledge Mr. R. Venkatraman's help in constructing the polygene. S.R. thanks TIFR for the VSRP fellowship. We also acknowledge Prof. G. Krishnamoorthy (TIFR) for helpful discussion. We thank Ms. Siddhi Inchanalkar for comments and critical reading of the manuscript.

REFERENCES

(1) Matouschek, A. *Curr. Opin. Struct Biol.* **2003**, *13*, 98.
(2) Prakash, S.; Matouschek, A. *Trends Biochem. Sci.* **2004**, *29*, 593.
(3) Maillard, R. A.; Chistol, G.; Sen, M.; Righini, M.; Tan, J.; Kaiser, C. M.; Hodges, C.; Martin, A.; Bustamante, C. *Cell* **2011**, *145*, 459.
(4) Onuchic, J. N.; Luthey-Schulten, Z.; Wolynes, P. G. *Annu. Rev. Phys. Chem.* **1997**, *48*, 545.
(5) Sali, A.; Shakhnovich, E.; Karplus, M. *Nature* **1994**, *369*, 248.
(6) Thirumalai, D.; Klimov, D. K.; Woodson, S. A. *Theor. Chem. Acc.* **1997**, *96*, 14.
(7) Wolynes, P. G.; Onuchic, J. N.; Thirumalai, D. *Science* **1995**, *267*, 1619.
(8) Zaidi, F. N.; Nath, U.; Udgaonkar, J. B. *Nat. Struct. Biol.* **1997**, *4*, 1016.
(9) Wright, C. F.; Lindorff-Larsen, K.; Randles, L. G.; Clarke, J. *Nat. Struct. Biol.* **2003**, *10*, 658.
(10) Jackson, G. S.; Hill, A. F.; Joseph, C.; Hosszu, L.; Power, A.; Waltho, J. P.; Clarke, A. R.; Collinge, J. *Biochim. Biophys. Acta* **1999**, *1431*, 1.
(11) Radford, S. E.; Dobson, C. M.; Evans, P. A. *Nature* **1992**, *358*, 302.
(12) Zhu, L.; Ghosh, K.; King, M.; Cellmer, T.; Bakajin, O.; Lapidus, L. J. *J. Phys. Chem. B* **2011**, *115*, 12632.
(13) Lapidus, L. J. *Curr. Opin. Struct. Biol.* **2013**, *23*, 30.
(14) Han, J. H.; Batey, S.; Nickson, A. A.; Teichmann, S. A.; Clarke, J. *Nat. Rev. Mol. Cell. Biol.* **2007**, *8*, 319.
(15) Vogel, C.; Bashton, M.; Kerrison, N. D.; Chothia, C.; Teichmann, S. A. *Curr. Opin. Struct. Biol.* **2004**, *14*, 208.
(16) Baldwin, R. L.; Rose, G. D. *Trends Biochem. Sci.* **1999**, *24*, 77.
(17) Udgaonkar, J. B. *Annu. Rev. Biophys.* **2008**, *37*, 489.
(18) Pirchi, M.; Ziv, G.; Riven, I.; Cohen, S. S.; Zohar, N.; Barak, Y.; Haran, G. *Nat. Commun.* **2011**, *2*, 493.
(19) Stigler, J.; Ziegler, F.; Gieseke, A.; Gebhardt, J. C.; Rief, M. *Science* **2011**, *334*, 512.
(20) Wang, Y.; Chu, X.; Suo, Z.; Wang, E.; Wang, J. *J. Am. Chem. Soc.* **2012**, *134*, 13755.
(21) Hoffmann, T.; Dougan, L. *Chem. Soc. Rev.* **2012**, *41*, 4781.

(22) Aggarwal, V.; Kulothungan, S. R.; Balamurali, M. M.; Saranya, S. R.; Varadarajan, R.; Ainavarapu, S. R. *J. Biol. Chem.* **2011**, *286*, 28056.
(23) Rief, M.; Gautel, M.; Oesterhelt, F.; Fernandez, J. M.; Gaub, H. E. *Science* **1997**, *276*, 1109.
(24) Carrion-Vazquez, M.; Oberhauser, A. F.; Fowler, S. B.; Marszalek, P. E.; Broedel, S. E.; Clarke, J.; Fernandez, J. M. *Proc. Natl. Acad. Sci. U.S.A.* **1999**, *96*, 3694.
(25) Best, R. B.; Fowler, S. B.; Herrera, J. L.; Steward, A.; Paci, E.; Clarke, J. *J. Mol. Biol.* **2003**, *330*, 867.
(26) Ainavarapu, S. R.; Li, L.; Badilla, C. L.; Fernandez, J. M. *Biophys. J.* **2005**, *89*, 3337.
(27) Brockwell, D. J.; Beddard, G. S.; Paci, E.; West, D. K.; Olmsted, P. D.; Smith, D. A.; Radford, S. E. *Biophys. J.* **2005**, *89*, 506.
(28) Hoffmann, T.; Tych, K. M.; Brockwell, D. J.; Dougan, L. *J. Phys. Chem. B* **2013**, *117*, 1819.
(29) Kotamarthi, H. C.; Sharma, R.; Koti Ainavarapu, S. R. *Biophys. J.* **2013**, *104*, 2273.
(30) Schwaiger, I.; Kardinal, A.; Schleicher, M.; Noegel, A. A.; Rief, M. *Nat. Struct. Mol. Biol.* **2004**, *11*, 81.
(31) Bertz, M.; Rief, M. *J. Mol. Biol.* **2008**, *378*, 447.
(32) Quiocho, F. A.; Ledvina, P. S. *Mol. Microbiol.* **1996**, *20*, 17.
(33) Magnusson, U.; Salopek-Sondi, B.; Luck, L. A.; Mowbray, S. L. *J. Biol. Chem.* **2004**, *279*, 8747.
(34) Indu, S.; Kochat, V.; Thakurela, S.; Ramakrishnan, C.; Varadarajan, R. *Proteins* **2011**, *79*, 244.
(35) Florin, E. L.; Rief, M.; Lehmann, H.; Ludwig, M.; Dornmair, C.; Moy, V. T.; Gaub, H. E. *Biosens. Bioelectron.* **1995**, *10*, 895.
(36) Marszalek, P. E.; Lu, H.; Li, H.; Carrion-Vazquez, M.; Oberhauser, A. F.; Schulten, K.; Fernandez, J. M. *Nature* **1999**, *402*, 100.
(37) Bustamante, C.; Marko, J. F.; Siggia, E. D.; Smith, S. *Science* **1994**, *265*, 1599.
(38) Peng, Q.; Li, H. *Proc. Natl. Acad. Sci. U.S.A.* **2008**, *105*, 1885.
(39) Ainavarapu, S. R.; Brujic, J.; Huang, H. H.; Wiita, A. P.; Lu, H.; Li, L.; Walther, K. A.; Carrion-Vazquez, M.; Li, H.; Fernandez, J. M. *Biophys. J.* **2007**, *92*, 225.
(40) Improta, S.; Politou, A. S.; Pastore, A. *Structure* **1996**, *4*, 323.
(41) Efron, B. *The Jackknife, the Bootstrap, and Other Resampling Plans*; Society for Industrial and Applied Mathematics: Philadelphia, PA, 1982.
(42) Onuchic, J. N.; Wolynes, P. G. *J. Chem. Phys.* **1993**, *98*, 2218.
(43) Huysmans, G. H.; Radford, S. E.; Baldwin, S. A.; Brockwell, D. J. *J. Mol. Biol.* **2012**, *416*, 453.
(44) Gao, X.; Qin, M.; Yin, P.; Liang, J.; Wang, J.; Cao, Y.; Wang, W. *Biophys. J.* **2012**, *102*, 2149.
(45) Mickler, M.; Dima, R. I.; Dietz, H.; Hyeon, C.; Thirumalai, D.; Rief, M. *Proc. Natl. Acad. Sci. U.S.A.* **2007**, *104*, 20268.
(46) He, C.; Genchev, G. Z.; Lu, H.; Li, H. *J. Am. Chem. Soc.* **2012**, *134*, 10428.
(47) Yu, H.; Liu, X.; Neupane, K.; Gupta, A. N.; Brigley, A. M.; Solanki, A.; Sosova, I.; Woodside, M. T. *Proc. Natl. Acad. Sci. U.S.A.* **2012**, *109*, 5283.
(48) Arad-Haase, G.; Chuartzman, S. G.; Dagan, S.; Nevo, R.; Kouza, M.; Mai, B. K.; Nguyen, H. T.; Li, M. S.; Reich, Z. *Biophys. J.* **2010**, *99*, 238.